



OPEN

Delay time of waves performing Lévy walks in 1D random media

L. A. Razo-López^{1,4}, A. A. Fernández-Marín¹, J. A. Méndez-Bermúdez¹, J. Sánchez-Dehesa² & V. A. Gopar³✉

The time that waves spend inside 1D random media with the possibility of performing Lévy walks is experimentally and theoretically studied. The dynamics of quantum and classical wave diffusion has been investigated in canonical disordered systems via the delay time. We show that a wide class of disorder—Lévy disorder—leads to strong random fluctuations of the delay time; nevertheless, some statistical properties such as the tail of the distribution and the average of the delay time are insensitive to Lévy walks. Our results reveal a universal character of wave propagation that goes beyond standard Brownian wave-diffusion.

A wave packet launched into a scattering region can penetrate that region and it may be reflected eventually. Thus, one might wonder how much time the wave packet has spent inside the media. This fundamental question was addressed by Wigner and Smith^{1,2}. It was shown that the delay time τ_R of a wave packet is related to the derivative of the reflection phase θ_R with respect to the frequency ω : $\tau_R = d\theta_R/d\omega$.

The delay time has received attention in many disciplines since it reveals information on the scattering medium and, therefore, it has also been of interest from an application point of view; e.g., the delay time is a fundamental quantity in imaging of tissues in optical coherence tomography^{3,4}.

A major issue in wave transport is the presence of disorder. Moreover, if waves propagate coherently through 1D random media, complex interference effects emerge, such as the widely studied phenomenon of Anderson localization^{5,6}: an exponential decay in space of classical and quantum waves, for instance, electromagnetic waves and electrons, respectively.

Since disorder is ubiquitous in real systems, there has been a great interest in studying the effects of Anderson localization on dynamical quantities such as the delay time. Microwave experiments have been performed to analyze statistical properties of wave dynamics^{7–9}, while several theoretical approaches have been developed to describe the delay-time statistics (see Ref.¹⁰ for a review).

Remarkably, it has been demonstrated that some statistical properties of the delay time are invariant in the sense that they are independent of the details of the medium. For instance, the inverse square power decay of the distribution of τ_R has been predicted in semi-infinite 1D systems¹¹ and also studied in higher dimensions^{12–14}. Another example is the average delay time, which is proportional to the mean length of trajectories¹⁵. This quantity was predicted to be invariant with respect to details of the scattering region, as recently observed experimentally^{15–17}.

Previous experimental and theoretical works on the delay time in 1D consider only models of disorder that lead to Anderson localization, however, there is a wide class of disorder—Lévy disorder—that leads to delocalization or anomalous localization, in relation to the Anderson localization^{18–21}. Anomalous localization finds its origin in the nonzero probability that waves travel a long distance without being scattered; these events are scarce but have a large impact. Such kind of events are sometimes called Lévy flights, however, the term Lévy flights is mostly used to study processes where the jumps or flights are instantaneous, while in Lévy walks, the velocity of the flights is constant, as in our study.

Here, we experimentally and theoretically study the delay time of reflected microwaves suffering coherent multiple scattering in a medium characterized by random spacings of scatterers following a one-sided Lévy α -stable distribution. Experiments in waveguides with standard disorder (i.e., with random scatterer separations following a non-heavy tailed distribution) are also performed to compare results with those of Lévy disorder. Additionally, numerical simulations are carried out to overcome some practical limitations of experiments and to obtain further support for our model. We calculate the distribution of the delay time and, furthermore, our

¹Instituto de Física, Benemérita Universidad Autónoma de Puebla, Apartado Postal J-48, Puebla 72570, Mexico. ²Departamento de Ingeniería Electrónica, Universitat Politècnica de València, Camino de vera s. n. (Edificio 7F), 46022 Valencia, Spain. ³Departamento de Física Teórica, Facultad de Ciencias, BIFI, Universidad de Zaragoza, Pedro Cerbuna 12, 50009 Zaragoza, Spain. ⁴Present address: Institut de Physique de Nice, CNRS, Université Côte d'Azur, Parc Valrose, 06100 Nice, France. ✉email: gopar@unizar.es

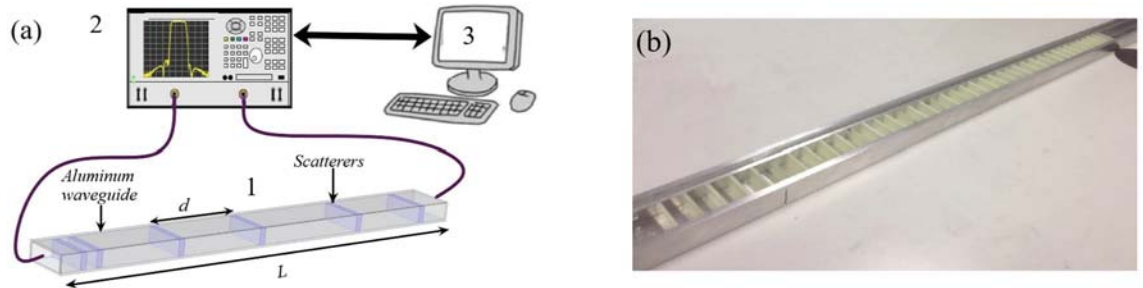


Figure 1. (a) Schematic view of the experimental setup. The aluminum waveguide (1), containing randomly distributed dielectric slabs, is connected to the ports of a vector network analyzer (2) and the data is stored in a computer (3). (b) Actual 2 m long aluminum waveguide (22.8 mm width and 10.6 mm height). The top is open to allow inner vision.

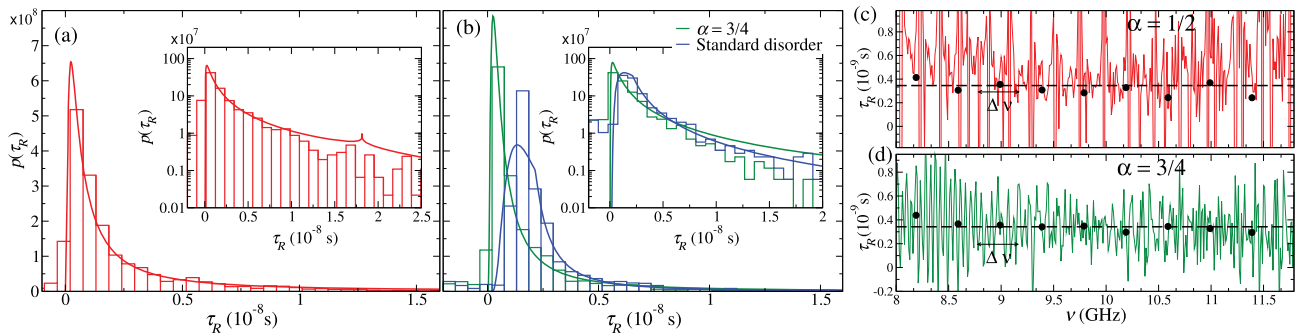


Figure 2. Experimental delay-time distributions (histograms) for Lévy waveguides characterized by (a) $\alpha = 1/2$ and $\langle -\ln T \rangle = 4.7$ at 9.9 GHz (red histogram) and (b) $\alpha = 3/4$ and $\langle -\ln T \rangle = 12$ at 11.2 GHz (green histogram). The blue histogram in (b) corresponds to random waveguides with ordinary (Gaussian) disorder with $\langle -\ln T \rangle = 12$ at 11.2 GHz. The histograms were constructed with (a) 4590 and (b) 1890 data. Insets show $p(\tau_R)$ on a logarithmic scale. Red, green (blue) solid curves show the theoretical predictions from Eq. (4) (Eq. (3)). Experimental delay times for a typical realization of the disorder of waveguides with (c) $\alpha = 1/2$ and (d) $3/4$. Black dots represent the average of τ_R over frequency windows $\Delta\nu = 0.4$ GHz. The horizontal black dashed lines are the averages of τ_R over the complete frequency window (8–12 GHz).

results allow us to conclude that universal features of the delay time in canonical disordered media go beyond standard Brownian models of wave diffusion, despite the fact that the presence of Lévy walks leads to stronger random fluctuations of the delay time.

Lévy statistics have been found in a broad range of contexts that go from foraging patterns of marine predators²² to fluctuations of stock market indices²³ or resonant emission of light²⁴. Lévy models are applied to describe anomalous diffusion of particles and waves that cannot be described by standard Brownian models^{25–32}.

Essentially, Lévy random processes are characterized by probability distributions whose tails decay like a power-law, i.e., if x is a random variable with probability density $\rho(x)$, then $\rho(x) \sim 1/x^{1+\alpha}$ for $x \gg 1$ ³³. Fluctuations of random variables that follow Lévy statistics are so large that the first and second moments diverge for $0 < \alpha < 1$.

Results

Experiments. Microwaves are launched into an aluminum waveguide containing 2.5 mm thick dielectric slabs whose separations follow a Lévy α -stable distribution (see Fig. 1). We work in a frequency range where a single transport channel is supported. Two different α -stable distributions characterized by their power-law decay have been chosen: $\alpha = 1/2$ and $3/4$. Additionally, a conventional disordered microwave waveguide with random spacing between slabs following a Gaussian distribution has been built. Using a network vector analyzer, we measure the 2×2 scattering matrix S :

$$S = \begin{pmatrix} \sqrt{R}e^{i\theta_R} & \sqrt{T}e^{i\theta_T} \\ \sqrt{T}e^{i\theta_T} & \sqrt{R}e^{i\theta_R'} \end{pmatrix}, \quad (1)$$

where R and T are the reflection and transmission coefficients, respectively. Measurements of S are thus collected over different disorder realizations.

From the collected S -matrices, we obtain τ_R and the probability distribution function $p(\tau_R)$. Figure 2a,b show the distribution $p_\alpha(\tau_R)$ with $\alpha = 1/2$ (red) and $3/4$ (green), respectively. The insets show $p_\alpha(\tau_R)$ on a logarithmic scale for a better visualization of the tail. In Fig. 2b, the delay-time distribution (blue histogram) for conventional

disorder is also shown. Both distributions in Fig. 2b have the same average value $\langle \ln T \rangle$. We can observe that the profile of both distributions (green and blue histograms) is different.

The distributions $p_\alpha(\tau_R)$ from our model, which we introduce below, are also shown (solid lines) in Fig. 2a,b. It is observed in Fig. 2a that for $\alpha = 1/2$, $p_\alpha(\tau_R)$ shows a small peak in the tail. The distribution for $\alpha = 3/4$ in Fig. 2b also exhibits a peak, but it is smoother and occurs at a larger value of τ_R , outside of the time range shown in Fig. 2b. We attribute these peaks to scattering processes that reach the right boundary of the waveguide; in Lévy disordered samples those processes are favored since waves can travel long distances without being scattered. In contrast, for ordinary disordered systems, $p(\tau_R)$ decays monotonically and for $\tau_R \gg 1$, $p(\tau_R) \sim 1/\tau_R^{21}$.

The trend of the experimental distributions (histograms) is well described by the model (solid lines), despite the fact that the statistics of τ_R is extracted from a limited amount of experimental data and the presence of a small tail for negative values of τ_R observed in Fig. 2a,b. Negative delay times are not considered in our model and are thus a source for discrepancies between experimental and theoretical results. It has been proposed that those negative values are due to a strong distortion of the wave packet produced due to interference between incident and promptly reflected waves^{34–37}.

We now address an invariance property of the mean path of trajectories with respect to the details of the disordered medium. This invariance property is equivalent to the independence of the average delay time with energy since both quantities are proportional¹⁵. To illustrate this invariance, in Fig. 2c,d, τ_R is plotted as a function of the linear frequency ν for typical samples with $\alpha = 1/2$ and $3/4$, respectively. We see strong fluctuations of τ_R , however, the average delay-time over frequency windows $\Delta\nu (= 0.4\text{GHz})$ is essentially independent of the frequency, as it is observed in both figures (dots). Moreover, the average over the whole frequency window (horizontal dashed line) has the same value ($3.4 \times 10^{-9}\text{s}$) for both cases: $\alpha = 1/2$ and $3/4$, and thus, it is independent of particularities of the medium. We will address this point later in more detail.

Model. For conventional disorder and within a random matrix approach to localization^{38,39}, the mean free path ℓ determines the statistical properties of the transport and it is related to the transmission by $s \equiv \langle -\ln T \rangle = L/\ell$, which is proportional to the number of scatterers n in the system, i.e., $\langle -\ln T \rangle = bn$ with b constant⁴⁰. If the random spacing between scatterers follows a Lévy α -stable distribution, the number of scatterers in a system of length L is subject to strong random fluctuations. Such fluctuations are described by the probability density $\Pi_L(n; \alpha)$ given by¹⁸: $\Pi_L(n; \alpha) = 2Lq_{\alpha,1}(L/(2n)^{1/\alpha})/\alpha(2n)^{(1+\alpha)/\alpha}$, where $q_{\alpha,c}(x)$ is the probability density function of the Lévy α -stable distribution with exponent α and scale parameter c . For $x \gg 1$, $q_{\alpha,c}(x) \sim c/x^{1+\alpha}$. Therefore, with the knowledge of $\Pi_L(n; \alpha)$ and the delay-time probability density for canonical disordered systems, $p_s(\tau_R)$, we write the probability density $p_\alpha(\tau_R)$ for Lévy disordered systems as

$$p_\alpha(\tau_R) = \int_0^\infty p_s(\tau_R) \Pi_L(n; \alpha) dn. \quad (2)$$

The probability density $p_s(\tau_R)$ in its full generality remains, however, an open problem. For semi-infinite disordered systems, assuming no transmission, the limit ($L \rightarrow \infty$) delay-time distribution $p_\infty(\tau_R)$ is given by^{11,41–45}: $p_\infty(\tau_R) = \tau_\ell \tau_R^{-2} \exp(-\tau_\ell/\tau_R)$, where τ_ℓ is the scattering time of the disorder. Real systems, however, are finite and finite-size effects may be of relevance. In particular, our experiments are performed in 2 m long waveguides and microwaves can be transmitted.

Our model for $p_s(\tau_R)$ that will be verified experimentally and numerically involves two main assumptions. Firstly, though the waves in our waveguides can be transmitted, we use a relationship between τ_R in the absence of absorption and R in the presence of weak absorption that assumes negligible transmission: $R = 1 - \tau_R/\tau_0$, where τ_0 is the absorption time which is assumed very large^{45–47}. A key point is that this relationship establishes that fluctuations of R determine the statistics of τ_R . Notice that for an ensemble of different samples, τ_0 fluctuates since it depends on the disorder configuration. Indeed, later τ_0 will be identified with $\langle \tau_R \rangle$, which contains information about the system length. Secondly, we use the Laguerre ensemble $p(\mu)$ which describes the statistics of R assuming large samples⁴⁸. We have verified that the Laguerre ensemble describes well our experimental results for the reflection of canonical disordered waveguides even though they are 2m long. See supplemental material (SM). That is, $p(\mu) \propto \exp(-\gamma\mu)$ where $\mu^{-1} \equiv R - 1$ and γ is a constant. For systems with absorption ($R < 1$) $\gamma < 0$ and $\mu < -1$, while for systems with amplification ($R > 1$), $\gamma > 0$ with $\mu > 0$. For the latter case $R = 1 + \tau_R/\tau_0$. Let us stress that for systems of finite length, τ_R can exceed τ_0 since, for instance, τ_R is infinite for transmitted waves. We thus need to consider both cases $\tau_R < \tau_0$ and $\tau_R > \tau_0$. Therefore, after the change of variable $\mu \rightarrow \tau_R$, the normalized distribution $p_s(\tau_R)$ can be expressed as

$$p_s(\tau_R) = \frac{a}{s[2 - \exp(-a/s)]} \frac{1}{\tau_R^2} \exp(-a|1/\tau_R - 1|/s), \quad (3)$$

where $a \equiv 2L/(\nu_g \tau_0)$ and ν_g is the group velocity. In writing Eq. (3), we conveniently measure the delay time in units of τ_0 , i.e., we replaced $\tau_R/\tau_0 \rightarrow \tau_R$. The above expression for $p_s(\tau_R)$ is obtained after making $\mu \rightarrow |\mu + 1|$ and the change of variable $\mu \rightarrow \tau_R$ in the Laguerre ensemble $p(\mu)$ with $-\mu^{-1} = 1 - R = \tau_R/\tau_0$. Notice that with the absolute value in Eq. (3), both cases $\tau_R/\tau_0 < 1$ and $\tau_R/\tau_0 > 1$ are considered. Our assumptions may overestimate $p_s(\tau_R)$, mainly for $\tau_R > \tau_0$, since some of the scattering processes that reach the right end of the

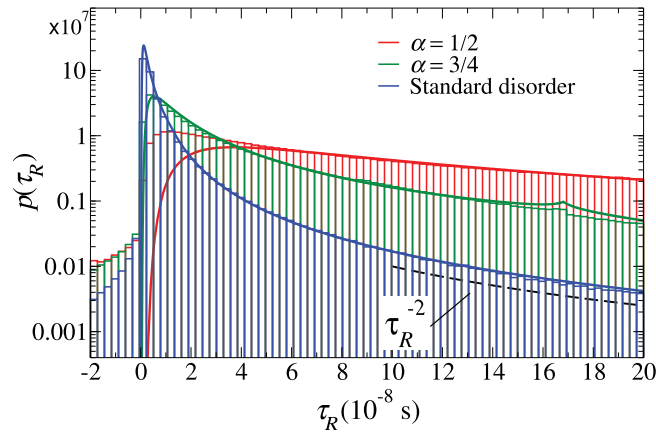


Figure 3. Numerical delay-time distributions with parameters $\alpha = 1/2$ (red histogram) and $\alpha = 3/4$ (green histogram) and for random waveguides with conventional (Gaussian) disorder (blue histogram). In all cases $\langle -\ln T \rangle = 10$. The histograms were constructed with 5×10^6 disorder realizations. The solid curves are the theoretical predictions from Eqs. (3) and (4) for standard and Lévy disorder, respectively. The dashed line, proportional to $1/\tau_R^2$, is a guide to the eye.

sample may leave the waveguide, having actually an infinite reflection delay time. Thus, as the systems become shorter, discrepancies between our model and experiments or simulations are expected. On the other hand, Eq. (3) reduces to $p_\infty(\tau_R)$ for $\tau_0/\tau_R \gg 1$. Additionally, since Eq. (3) is based on the Laguerre ensemble, in the SM we have experimentally and numerically verified the distribution of the reflection coefficient predicted by the Laguerre ensemble.

We now define $s(z, \alpha, \xi) \equiv \xi/(2z^\alpha f(\alpha))$ with $z = L/(2n)^{1/\alpha}$ and, for a system of fixed L , $\xi = \langle -\ln T \rangle_L$ which is given by¹⁸: $\langle -\ln T \rangle_L = bL^\alpha f(\alpha)/c$, where $f(\alpha) = (1/2) \int_0^\infty z^{-\alpha} q_{\alpha,1}(z) dz$. Therefore, using Eqs. (2) and (3), we write the distribution of τ_R for Lévy disordered samples as

$$p_\alpha(\tau_R) = \int_0^\infty p_{s(z, \alpha, \xi)}(\tau_R) q_{\alpha,1}(z) dz, \quad (4)$$

where $p_{s(z, \alpha, \xi)}(\tau_R)$ is given in Eq. (3) with s replaced by $s(z, \alpha, \xi)$. The experimental distributions in Fig. 2 have been compared with Eqs. (3, 4) using τ_0 as a fitting parameter.

Numerical simulations are now performed for further support of Eq. (4) and to reveal universal properties. Thus, the number of disorder realizations is greatly increased and absorption, which reduce the effects of long trajectories, is absent. Details of the numerical simulations are provided in the SM.

Figure 3 compares numerical and theoretical delay time distributions from Eqs. (3) and (4) for standard and Lévy disordered waveguides with $\alpha = 1/2$ and $3/4$ and $\xi = 10$. For conventional disorder, our simulations show a physically meaningful result: the absorption time τ_0 can be identified with the average $\langle \tau_R \rangle$. After this identification, since $\langle \tau_R \rangle$ can be extracted from the numerical simulations, there is no free fitting parameters in Eq. (3). Similarly, for Lévy disorder τ_0 has been found to fit the numerical distributions with $\tau_0 = 2\langle \tau_R \rangle/\alpha$ (for the standard disorder, $\alpha = 2$). This result is appealing, however, its formal demonstration remains as an open problem.

Although the distribution profiles in Fig. 3 are different and show the impact of Lévy walks, they share some properties that are not evident because of the different time scale of each case.

In order to compare $p_\alpha(\tau_R)$ for different system parameters, it is convenient to express τ_R in units of $2L/v_g$, as shown in Fig. 4 for $\alpha = 1/2$ and $3/4$, left and right panels, respectively, and $\xi = 10$ and 4 , upper and lower panels, respectively. A notorious difference with respect to the distribution for standard disordered systems (Fig. 3, blue line) is that a peak appears at $\tau_R/(2L/v_g) = 1$, which is precisely the time that a wave would spend on traveling back and forth between the boundaries of the waveguide in the absence of disorder.

For shorter systems (Fig. 4c,d), we notice a deviation, mainly at the distribution tails, of the theoretical predictions (solid lines) with respect to the numerical results. Also, the numerical simulations start to deviate from the $1/\tau_R^2$ decay (see insets in Fig. 4c,d), which is expected since the transmission is higher as the waveguide becomes shorter.

We now show that some properties of τ_R go beyond canonical disorder models. We have already mentioned the inverse square decay of the delay time distributions for $\tau_R \gg 1$ obtained in 1D semi-infinite Anderson localized systems; indeed, such power-law behavior has been explained by resonance models in the localized regime^{11,44,49}. For Lévy disordered structures, the insets of Fig. 4a,b compare the tail of the distributions for $\alpha = 1/2$ and $3/4$, respectively, with $1/\tau_R^2$ decay (dashed lines); see also the SM for further details and numerical fits of the tails. Actually, from Eqs. (3) and (4), we also find that $p_\alpha(\tau_R) \sim 1/\tau_R^2$ for $\tau_R \gg 1$.

Additionally, the average $\langle \tau_R \rangle$ is a linear function of the system length: $\langle \tau_R \rangle = L/v_g$, as shown in Fig. 5a for $\alpha = 1/2$ and $3/4$ (inset), which is also observed in standard disordered systems^{11,43}. Furthermore, an interesting invariance property of the mean length of random walk trajectories with respect to the details of the disorder¹⁶ has been recently investigated in optical experiments¹⁷. The invariance of the mean path length is equivalent to

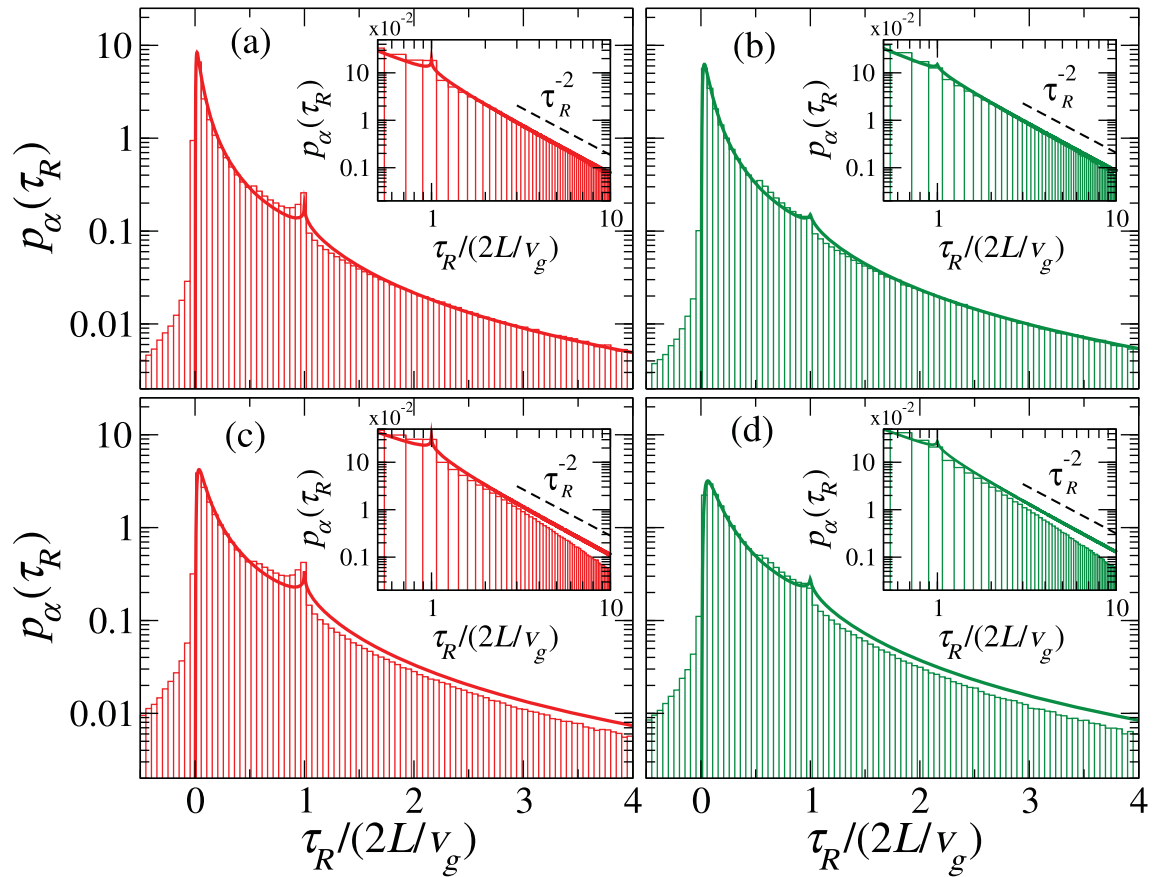


Figure 4. Numerical distributions $p_\alpha(\tau_R)$ (histograms) for Lévy disordered systems characterized by (a,c) $\alpha = 1/2$ and (b,d) $\alpha = 3/4$ with (a,b) $\xi = 10$ and (c,d) $\xi = 4$. Each histogram was obtained from 5×10^6 disorder realizations. The solid curves are the theoretical predictions from Eq. (4). Insets show $p_\alpha(\tau_R)$ in a logarithmic scale. The dashed lines, following the power law $1/\tau_R^2$, are a guide to the eye (see also SM).

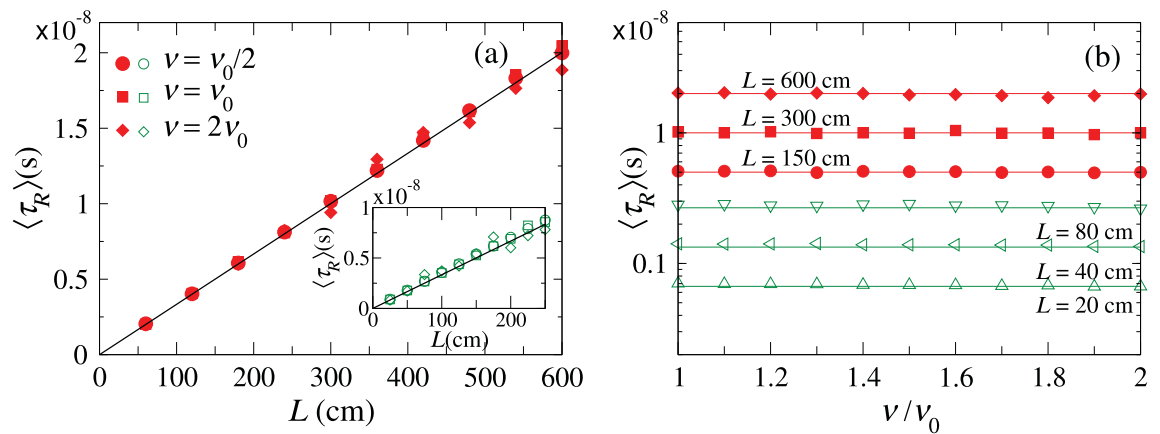


Figure 5. (a) Numerical average delay-time $\langle \tau_R \rangle$ for Lévy disorder as a function of the length L for different linear frequencies ν ($\nu_0 = 7.5$ GHz) with $\alpha = 1/2$ (main frame) and $\alpha = 3/4$ (inset). (b) $\langle \tau_R \rangle$ as a function of ν for several lengths L for $\alpha = 1/2$ (red symbols) and $\alpha = 3/4$ (green symbols). The averages are obtained from 10^5 disorder realizations. The horizontal solid lines correspond to $\langle \tau_R \rangle = L/\nu_g$ in each case.

the independence of the average delay-time to the energy. We have already shown experimental evidence of this invariance in Fig. 2c,d. Figure 5b provides additional numerical evidence by showing $\langle \tau_R \rangle$ for disordered systems of different lengths with $\alpha = 1/2$ and $3/4$. We observe that $\langle \tau_R \rangle$ is constant with the linear frequency ν . Thus, these results give further evidence that the invariance of the mean path length goes beyond Brownian random walk models. This invariance can be explained by a direct relation between the delay time and the density of states², as was studied in¹⁵ from ballistic to localized regimes.

Discussion

We have studied experimentally and theoretically the impact of Lévy walks on a fundamental dynamical quantity: the delay time. Although the delay-time distributions for Lévy and canonical disordered structures are different, remarkably, some properties are invariant, e.g., the inverse square power-law decay of the delay-time distribution and the insensitivity of the average delay time to energy. The latter is equivalent to the invariance of the mean path length observed in experiments of light propagation. Additionally, the linear dependence of the average delay time with the length in ordinary disordered media is not affected by the presence of Lévy walks. Altogether, our results reveal a universal character of wave propagation that goes beyond standard Brownian models^{15–17}.

We point out that in Lévy disordered systems with $\alpha < 1$, the mean free path is meaningless since it diverges, in contrast to canonical disordered systems in which the mean free path settles the wave statistics. In the presence of Lévy type of disorder, two quantities determine the transport statistics: α and the logarithmic transmission average.

Our model shows a good agreement with experimental and numerical results, however, only structures with a single transport channel or 1D systems have been considered. Although nowadays 1D wave transport is of relevance, it would be desirable to extend our study to higher dimensions. Nevertheless, the ideas and results presented here are so general that they can be applied from classical to quantum waves in disordered media.

Methods

To determinate experimentally the delay times τ_R , we employ the experimental setup schematically described in Fig. 1. We use a 2 meters long aluminum waveguide with a rectangular cross-section (22.8 mm width and 10.6 mm height) in which we insert a random distribution of dielectric scatterers. Each scatterer consists of a 2.5 mm thick dielectric slab. The slabs are made of FR4, a composite material with low losses, its dielectric permittivity is $\epsilon = 4.4 + i0.088$.

With those dimensions of the waveguide, the fundamental mode TE₁₀ propagates along the waveguide in the frequency range from 7.5 to 15 GHz. Within this frequency window, the waveguide can be effectively considered as a 1D random waveguide. A two-port vector network analyzer (VNA) ZVA 24 from Rohde & Schwarz (2 in Fig. 1) with a resolution of 1 Hz is employed to generate and receive microwave signals in the region of interest. The ports of the VNA are used alternatively as sources and receivers of the microwave signals. Each port is connected to the aluminum waveguide by means of standard X-band microwave transitions placed at both sides of the waveguide. This allows the measurements of the four matrix elements of the complex S-matrix, $S(v)$, where v is the linear frequency. In particular, the phase of the reflection amplitude $\theta_R(v)$ is obtained as given in Eq. (1).

From the set of measured phases $\theta_R(v_i)$, we compute the delay times $\tau_R(v) = d\theta_R(v)/d\omega$ as

$$\tau_R(v_i) \approx \frac{1}{2\pi} \frac{\theta_R(v_{i+1}) - \theta_R(v_i)}{\Delta v},$$

where $\Delta v = (v_{i+1} - v_i) = 0.01\text{GHz}$.

We have built waveguides with both Lévy and canonical types of disorder. For the Lévy waveguides, the dielectric slabs have been placed accordingly to a α -stable distribution with parameters $\alpha = 1/2$ and $3/4$, i.e., $\rho(d) \sim 1/d^{1+\alpha}$ for $d \gg 1$. Let us comment that in general there are no closed-form expressions in terms of elementary functions for the Lévy α -stable distributions. An explicit closed expression for $q_{\alpha,c}(x)$ can be conveniently given using the Fourier transform⁵⁰: $\tilde{q}_{\alpha,c}(k) = \exp[-|k|^\alpha (BH(k) + \bar{B}H(-k))]$, where H is the Heaviside step function and \bar{B} is the complex conjugate of $B = -c\Gamma(-\alpha) \exp(i\pi\alpha/2)$, Γ being the Gamma function. For any value of α with $0 < \alpha < 2$, the Lévy α -stable distribution is generated numerically³³.

For the canonical disorder, the separation between slabs follows a standard normal distribution (zero mean and unit variance).

An ensemble of 135 random waveguides of different disorder realizations have been built for each case: $\alpha = 1/2$, $3/4$, and standard disorder. We measured the reflection amplitude in a frequency window centered at $v = 9.9\text{GHz}$ for Lévy disordered waveguides with $\alpha = 1/2$. For $\alpha = 3/4$ and for conventional disorder, the reflection amplitude was measured in a frequency window centered at $v = 11.2\text{GHz}$. Thus, the experimental histograms of Fig. 2a,b have been obtained from 4590 and 1890 delay times, respectively.

Received: 17 September 2020; Accepted: 17 November 2020

Published online: 30 November 2020

References

1. Wigner, E. P. Lower limit for the energy derivative of the scattering phase shift. *Phys. Rev.* **147**, 145–147 (1955).
2. Smith, F. T. Lifetime matrix in collision theory. *Phys. Rev.* **119**, 2098–2098 (1960).
3. Fercher, A. F., Drexler, W., Hitzinger, C. K. & Lasser, T. Optical coherence tomography - principles and applications. *Rep. Prog. Phys.* **66**, 239–303 (2003).
4. Lubatsch, A. & Frank, R. Self-consistent quantum field theory for the characterization of complex random media by short laser pulses. *Phys. Rev. Res.* **2**, 013324 (2020).
5. Anderson, P. W. Absence of diffusion in certain random lattices. *Phys. Rev.* **109**, 1492–1505 (1958).

6. Lagendijk, A., van Tiggelen, B. & Wiersma, D. S. Fifty years of Anderson localization. *Phys. Today* **62**, 24–29 (2009).
7. Genack, A. Z., Sebbah, P., Stoytchev, M. & van Tiggelen, B. A. Statistics of wave dynamics in random media. *Phys. Rev. Lett.* **82**, 715–718 (1999).
8. Sebbah, P., Legrand, O. & Genack, A. Z. Fluctuations in photon local delay time and their relation to phase spectra in random media. *Phys. Rev. E* **59**, 2406–2411 (1999).
9. Chabanov, A. A. & Genack, A. Z. Statistics of dynamics of localized waves. *Phys. Rev. Lett.* **87**, 233903 (2001).
10. Texier, C. Wigner time delay and related concepts: Application to transport in coherent conductors. *Phys. E Low. Dimens. Syst. Nano Struct.* **82**, 16–33 (2016).
11. Texier, C. & Comtet, A. Universality of the Wigner time delay distribution for one-dimensional random potentials. *Phys. Rev. Lett.* **82**, 4220–4223 (1999).
12. Schomerus, H., van Bommel, K. J. H. & Beenakker, C. W. J. Coherent backscattering effect on wave dynamics in a random medium. *EPL* **52**, 518–524 (2000).
13. Xu, F. & Wang, J. Statistics of Wigner delay time in Anderson disordered systems. *Phys. Rev. B* **84**, 024205 (2011).
14. Ossipov, A. Scattering approach to Anderson localization. *Phys. Rev. Lett.* **121**, 076601 (2018).
15. Pierrat, R. *et al.* Invariance property of wave scattering through disordered media. *Proc. Natl Acad. Sci. USA* **111**, 17765–17770 (2014).
16. Blanco, S. & Fournier, R. An invariance property of diffusive random walks. *EPL* **61**, 168–173 (2003).
17. Savo, R. *et al.* Observation of mean path length invariance in light-scattering media. *Science* **358**, 765–768 (2017).
18. Falceto, F. & Gopar, V. A. Conductance through quantum wires with Lévy-type disorder: Universal statistics in anomalous quantum transport. *EPL* **92**, 57014 (2010).
19. Amanatidis, I., Klefogiannis, I., Falceto, F. & Gopar, V. A. Conductance of one-dimensional quantum wires with anomalous electron wave-function localization. *Phys. Rev. B* **85**, 235450 (2012).
20. Klefogiannis, I., Amanatidis, I. & Gopar, V. A. Conductance through disordered graphene nanoribbons: Standard and anomalous electron localization. *Phys. Rev. B* **88**, 205414 (2013).
21. Lima, J. R. F., Pereira, L. F. C. & Barbosa, A. L. R. Dirac wave transmission in Lévy-disordered systems. *Phys. Rev. E* **99**, 032118 (2019).
22. Mantegna, R. N. & Stanley, H. E. Scaling behaviour in the dynamics of an economic index. *Nature* **376**, 46–49 (1995).
23. Reynolds, A. M. & Ouellette, N. T. Swarm dynamics may give rise to Lévy flights. *Sci. Rep.* **6**, 30515 (2016).
24. Patel, R. & Mehta, R. V. Lévy distribution of time delay in emission of resonantly trapped light in ferrodistributions. *J. Nanophoton.* **6**, 069503 (2012).
25. Bouchaud, J.-P. & Georges, A. Anomalous diffusion in disordered media: statistical mechanisms, models and physical applications. *Phys. Rep.* **195**, 127 (1990).
26. Shlesinger, M. F., Klafter, J. & Zumofen, G. Above, below and beyond brownian motion. *Am. J. Phys.* **67**, 1253–1259 (1999).
27. Barkai, E., Fleurov, V. & Klafter, J. One-dimensional stochastic Lévy-Lorentz gas. *Phys. Rev. E* **61**, 1164–1169 (2000).
28. Barthelmy, P., Bertolotti, J. & Wiersma, D. A Lévy flight for light. *Nature* **453**, 495–498 (2008).
29. Solomon, T. H., Weeks, E. R. & Swinney, H. L. Observation of anomalous diffusion and Lévy flights in a two-dimensional rotating flow. *Phys. Rev. Lett.* **71**, 3975–3978 (1993).
30. Mercadier, N., Guerin, W., Chevrollier, M. & Kaiser, R. Lévy flights of photons in hot atomic vapours. *Nat. Phys.* **5**, 602–605 (2009).
31. Rocha, E. G. *et al.* Lévy flights for light in ordered lasers. *Phys. Rev. A* **101**, 023820 (2020).
32. Zaburdaev, V., Denisov, S. & Klafter, J. Lévy walks. *Rev. Mod. Phys.* **87**, 483–530 (2015).
33. Uchaikin, V. V. & Zolotarev, V. M. *Chance and Stability. Stable Distributions and Their Applications.* (VSP, Utrecht, 1999).
34. Garrett, C. & McCumber, D. Propagation of a Gaussian light pulse through an anomalous dispersion medium. *Phys. Rev. A* **1**, 305–313 (1970).
35. Dalitz, R. H. & Moorhouse, R. G. What is a resonance?. *Proc. R. Soc. Lond. Ser. A* **318**, 279 (1970).
36. Chu, S. & Wong, S. Linear pulse propagation in an absorbing medium. *Phys. Rev. Lett.* **48**, 738–741 (1982).
37. Durand, M., Popoff, S. M., Carminati, R. & Goetschy, A. Optimizing light storage in scattering media with the dwell-time operator. *Phys. Rev. Lett.* **123**, 243901 (2019).
38. Anderson, P. W., Thouless, D. J., Abrahams, E. & Fisher, D. S. New method for a scaling theory of localization. *Phys. Rev. B* **22**, 3519–3526 (1980).
39. Mello, P. & Kumar, N. *Quantum Transport in Mesoscopic Systems: Complexity and Statistical Fluctuation* (Oxford University Press, Oxford, 2004).
40. Mello, P. A. Central-limit theorems on groups. *J. Math. Phys.* **27**, 2876–2891 (1986).
41. Jayannavar, A. M., Vijayagovindan, G. V. & Kumar, N. Energy dispersive backscattering of electrons from surface resonances of a disordered medium and 1/f noise. *Z. Phys. B Condens. Matter* **75**, 77–79 (1989).
42. Heinrichs, J. Invariant embedding treatment of phase randomisation and electrical noise at disordered surfaces. *J. Phys. Condens. Matter* **2**, 1559–1568 (1990).
43. Comtet, A. & Texier, C. On the distribution of the Wigner time delay in one-dimensional disordered systems. *J. Phys. A: Math. Gen.* **30**, 8017–8025 (1997).
44. Bolton-Heaton, C. J., Lambert, C. J., Falko, V. I., Prigodin, V. & Epstein, A. J. Distribution of time constants for tunneling through a one-dimensional disordered chain. *Phys. Rev. B* **60**, 10569–10572 (1999).
45. Beenakker, C. W. J. *Dynamics of Localization in a Waveguide*, 489–508 (Springer, Netherlands, 2001).
46. Klyatskin, V. I. & Saichev, A. I. Statistical and dynamic localization of plane waves in randomly layered media. *Sov. Phys. Uspekhi* **35**, 231–247 (1992).
47. Anantha Ramakrishna, S. & Kumar, N. Imaginary potential as a counter of delay time for wave reflection from a one-dimensional random potential. *Phys. Rev. B* **61**, 3163–3165 (2000).
48. Beenakker, C. W. J., Paasschens, J. C. J. & Brouwer, P. W. Probability of reflection by a random laser. *Phys. Rev. Lett.* **76**, 1368–1371 (1996).
49. Kottos, T. Statistics of resonances and delay times in random media: beyond random matrix theory. *J. Phys. A: Math. Gen.* **38**, 10761–10786 (2005).
50. Calvo, I., Cuchi, J. C., Esteve, J. G. & Falceto, F. Generalized central limit theorem and renormalization group. *J. Stat. Phys.* **141**, 409 (2010).

Acknowledgements

A. A. F.-M. thanks the hospitality of the Laboratoire d’Acoustique de l’Université du Mans, France, where part of this work was done. J. A. M.-B. gratefully acknowledges to Departamento de Matemática Aplicada e Estatística, Instituto de Ciências Matemáticas e de Computação, Universidade de São Paulo during which this work was completed. J.A.M.-B. was supported by FAPESP (Grant No. 2019/06931-2), Brazil. A. A. F.-M. thanks partial support by RFI Le Mans Acoustique and by the project HYPERMETA funded under the program Étoiles

Montantes of the Region Pays de la Loire. V. A. G. acknowledges support by MCIU (Spain) under the Project number PGC2018-094684-B-C22.

Author contributions

L.A.R.-L. performed the numerical simulations. A.A.F.-M. and J.S.-D. conducted and designed the experiments. L.A.R.-L., J.A.M.-B., and V.A.G. analyzed the results and contributed to the preparation of the manuscript. All authors reviewed the manuscript.

Competing interests

The authors declare no competing interests.

Additional information

Supplementary information is available for this paper at <https://doi.org/10.1038/s41598-020-77861-x>.

Correspondence and requests for materials should be addressed to V.A.G.

Reprints and permissions information is available at www.nature.com/reprints.

Publisher's note Springer Nature remains neutral with regard to jurisdictional claims in published maps and institutional affiliations.



Open Access This article is licensed under a Creative Commons Attribution 4.0 International License, which permits use, sharing, adaptation, distribution and reproduction in any medium or format, as long as you give appropriate credit to the original author(s) and the source, provide a link to the Creative Commons licence, and indicate if changes were made. The images or other third party material in this article are included in the article's Creative Commons licence, unless indicated otherwise in a credit line to the material. If material is not included in the article's Creative Commons licence and your intended use is not permitted by statutory regulation or exceeds the permitted use, you will need to obtain permission directly from the copyright holder. To view a copy of this licence, visit <http://creativecommons.org/licenses/by/4.0/>.

© The Author(s) 2020